2021 IEEE/ASME International Conference on
Advanced Intelligent Mechatronics (AIM)

Preliminary Study of Pressure Self-Sensing Miniature Magnetorheological Valves

Sofia Lydia Ntella, Kenny Jeanmonod, Minh-Trung Duong, Yoan Civet, Christian Koechli, Yves Perriard[1]

2021 IEEE/ASME International Conference on Advanced Intelligent Mechatronics (AIM) | 978-1-6654-4139-1/21/$31.00 ©2021 IEEE | DOI: 10.1109/AIM46487.2021.9517656

***Abstract*—Magnetorheological (MR) valves have been included in many innovative engineering systems, such as dampers, clutches, or brakes, with different fields of application. Their role serves actuation purposes, while integrated displacement and velocity sensing in the actuators has been studied, as well. In this paper, we present the working principle, design, and preliminary results of a miniature MR valve with pressure self-sensing capabilities that exploits the electromagnetic induction phenomenon. The valve can work in a pressure range from $200\ kPa$ to $700\ kPa$, supplied by a current of a maximum $0.3\ A$. The suggested valve design is realized with two coils, one for the current application and the magnetic field creation and one for the sensing of the electromagnetic induction. A specially designed test-bench, that facilitates MR fluid flow and pressure regulation, was used for the experimental procedures.**

***Index Terms*—MR valve, pressure self-sensing, electromagnetic induction**

I. Introduction

In the last two decades, MR devices have attracted the interest of many researchers and have been incorporated into a wide range of applications. Some examples include industrial procedures such as product gripping and handling [1], or transportation lines [2], medical applications for joint orthoses [3], [4], haptic devices [5], [6] or applications in automotive industry [7]. The devices contain a smart fluid, called MR fluid. The material's intelligence is based on the fact that a magnetic field excitation on it leads to a reversible increase of the fluid viscosity [8]. This principle, together with other important characteristics of MR fluids, such as low power consumption and fast response time [9] are used for the design of several MR devices, for instance, dampers [10], clutches [11], brakes [12] or valves [13], [14].

In the case of MR valves, the structure includes a path through which the MR fluid can flow. The application of the magnetic field and, thus, the increase of the MR fluid viscosity, blocks the fluid path, closing the valve. On the contrary, when no field exists, the fluid can flow and the MR valve is considered open. This allows the function of the valve in two states, the on-state (closed valve) and the off-state (open valve), facilitating actuation applications. In parallel with the two-state functionality, the self-sensing abilities of the MR valves have intrigued some researchers. The existing studies focus on measuring quantities such as displacement or velocity in MR dampers. The dampers are part of vibration systems and the sensed value is used as feedback for the controller of these systems [15], [16], [17]. In these papers, the authors provide a combination of DC and AC current to the exciting coil. The structures include not only the main excitation coil but also additional sensing coils. The DC current on the excitation coil creates the MR effect and the blocking of the valve, while the AC current is responsible for the alternating, self-induced voltages on the additional coils. The induced voltages are related to the displacement and velocity of the piston of the structure. Although, these devices present self-sensing capabilities concerning displacement and velocity, they have not been studied concerning pressure self-sensing. At the same time, the additional coils, as well as the need for an alternating current for the voltage induction increase the complexity, the size, and the power consumption of the MR devices.

In the current study, we present a miniature MR valve with a simple structure that utilizes two coils and acts as a combination of sensor and actuator. However, in contrast with the previous studies, it is powered only by DC current for both the magnetization of the fluid particles and the voltage induction. The electromagnetic induction phenomenon appears due to the change of the magnetic circuit properties when pressure is applied on the MR fluid. In addition, the novel miniature MR device that we propose presents both actuating and pressure sensing possibilities, with further potential for displacement and velocity self-sensing.

II. MR Valve

A. Actuation Principle

MR valves consist, as in Fig. 1, of a ferromagnetic inner core, around which the exciting coil is wound and a ferromagnetic outer core. Between the inner and the outer part, there exists a gap that allows the flow of the MR fluid. The fluid consists of micron-sized ferromagnetic particles contained in a carrier medium, which is usually oil. A magnetic field excitation leads to the alignment of the particles across the magnetic poles, forming chain-like structures. In that event, there is a shift in the fluid state from liquid to semi-solid. In our case, we opted for an annular valve model, due to its simplicity that facilitates fabrication and testing. When a DC current is applied to the coil, a magnetic field is created and the particle chains are formed in parallel with the magnetic field sense in the active regions of the structure. The chain formation, which is reversible, leads to the increase of the fluid viscosity and the blocking of the valve. In this work, we use two coils instead of one, which is included in the traditional MR valve structure, to employ the exciting coil for the magnetic field application and the sensing coil for the electromagnetic induction phenomenon that will be explained below.

[1]The authors are with the Integrated Actuators Laboratory (LAI), École Polytechnique Fédérale de Lausanne (EPFL), Neuchâtel, Switzerland sofia.ntella@epfl.ch

At low magnetic field values, the magnetic flux density B is written as a function of magnetic field intensity H:

$$B = \mu_0 \mu_r H \tag{1}$$

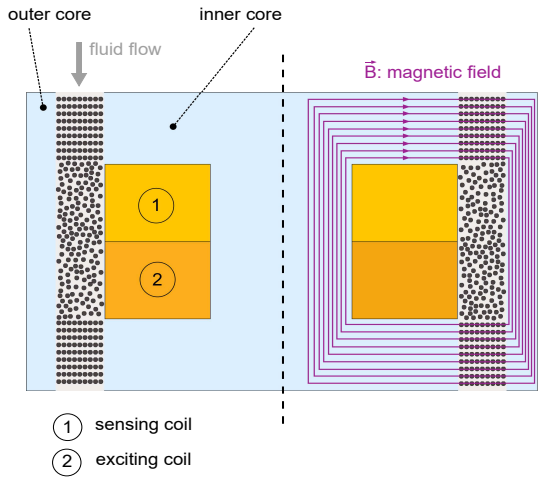

Fig. 1: Structure of a magnetorheological valve with two coils in a 2-D cross-section plane.

The variation of the magnetic field perpendicularly to the fluid path leads to the variation of the fluid yield stress τ_y, which controls the fluid resistance to flow. Between the points, where the fluid enters and exits the gap, if we assume a one-direction flow from the top to the bottom, a pressure drop appears which is dependent on two factors, the magnetic field, and the viscosity, and can be described by the following equation [13], where c is a parameter ranging from 2 to 3 [13], η is the fluid viscosity, and h_t, g, r_i are the valve dimensions shown in Fig. 2(a):

$$\Delta P = \Delta P_\tau + \Delta P_\eta = \frac{c\tau_y(H)2h_t}{g} + \frac{6\eta Q 2h_t}{g^3(r_i+g)\pi} \tag{2}$$

B. Pressure Self-Sensing Phenomenon

When the exciting current remains at low levels, the ferromagnetic particles form loose bonds with each other and as a result, the chain-like structures are weak enough and their shape can be altered in the presence of external factors, such as pressure. When pressure is applied on one side of the valve as in Fig. 2(a), the chains of the MR fluid with initial length l_g tend to elongate to a higher length l'_g. Fig. 2(b) depicts the magnetic circuit equivalent of a 2-D axis-symmetric cross-section of the valve. $\mathcal{R}_1$, $\mathcal{R}_2$ and $\mathcal{R}_{MR}$ are the magnetic reluctances of the outer core the inner core, and the MR fluid in the gap respectively. The elongation brings about changes in the magnetic circuit, by varying the quantity $\mathcal{R}_{MR} = l_g/(\mu_{MR}S)$, which is proportional to the length of the gap and inversely proportional to the permeability of the MR fluid and the cross-section surface of the gap. To calculate the pressure drop and study the way the applied pressure affects the chain-like structures, the magnetic circuit equations of the valve are solved and presented below. According to Ampere's law, for the closed magnetic path C (Fig. 2(a)), we have:

$$N \cdot I = \oint_C \mathbf{H} \cdot d\mathbf{l} \tag{3}$$

where N is the number of turns of the exciting coil, I is the current applied to the coil, and H is the magnetic field intensity on the effective length dl of the magnetic path. Using the dimensions of Fig. 2(a), Eq. (3) can be written as:

$$\begin{aligned} N \cdot I = {} & 2H_g l_g \\ & + H_{o1}(h - h_t) + H_{o2} 2\frac{(r_o - g - r_i)}{2}) \\ & + H_{i1}(h - h_t) + H_{i2}(2w_c + 2\frac{r_i - w_c}{2}) \end{aligned} \tag{4}$$

where H_g is the magnetic field intensity in the gap, H_{o1} and H_{o2} is the magnetic field intensity for the corresponding magnetic path in the outer core and H_{i1} and H_{i2} is the magnetic field intensity for the corresponding path in the inner core.

Moreover, due to the magnetic flux conservation rule in the magnetic circuit, and assuming no leakage exists, we have:

$$\Phi_g = \Phi_o = \Phi_i \Rightarrow B_g S_g = B_o S_o = B_i S_i \tag{5}$$

where μ_0 is the magnetic permeability of free space and μ_r is the relative permeability of each material. After solving Eq. (4), using Eq. (1) and Eq. (5) and acquiring Φ_g and B_g, we can conclude that the magnetic flux Φ_g in the gap is correlated to the length of the particle chains. Thus, an abrupt application of pressure on the chain structure can lead to elongation and, consequently, to variation of the magnetic path of the circuit and the magnetic flux in the gap. The flux can also be written as a function of the magnetic reluctance of the MR fluid $\mathcal{R}_{MR}$ [18]:

$$\Phi(t) = \frac{N \cdot i}{\mathcal{R}_{MR}} \tag{6}$$

$$\mathcal{R}_{MR} = \frac{ln(1 + \frac{l_g}{r_i})}{\pi h_t \mu_0 \mu_{MR}} \tag{7}$$

where l_g is the chains' length and μ_{MR} is the MR fluid relative permeability. Since $r_g >> l_g$, we can simplify Eq. (7) as follows:

$$\mathcal{R}_{MR} = \frac{l_g(t)}{\pi r_i h_t \mu_0 \mu_{MR}} \tag{8}$$

The variation of magnetic flux in the gap leads to the appearance of an induced voltage:

$$\mathcal{E} = -N \cdot \frac{d\Phi}{dt} \tag{9}$$

The theoretical analysis can prove the voltage induction on the sensing coil of the MR valve. Further, if we transform Eq. (9) as follows, with P being the applied pressure on the MR fluid, we can involve the applied pressure in the analytical solution:

$$\mathcal{E} = -N \cdot \frac{d\Phi}{dP} \cdot \frac{dP}{dt} \tag{10}$$

The experimental trials aim at proving the correlation between the induced voltage and the pressure sensed by the valve.

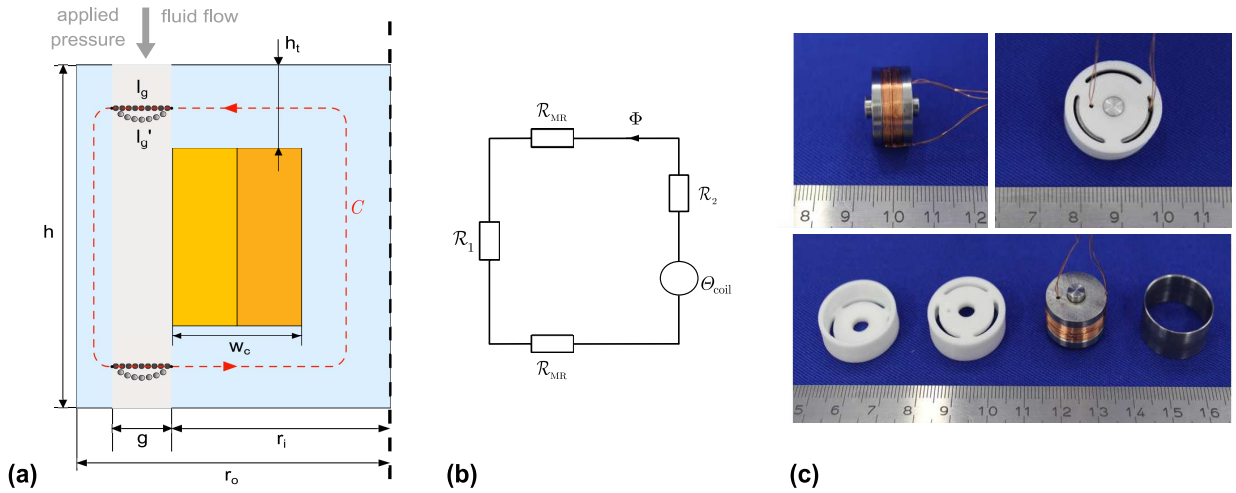

Fig. 2: (a) The magnetic path in a 2-D cross-section of the MR valve, and elongation of chains with pressure application (b) Magnetic circuit equivalent (c) Fabricated MR valve with two coils and plastic protection holder.

C. Valve Design

The MR valve was designed and its magnetic behavior was simulated using Flux 2019. The magnetic cores - inner and outer - were fabricated by soft iron made by ARMCO. The dimensions h, h_t, g, r_i, and r_o of the valve are displayed in Table I and Fig. 2(a), while the valve prototype is depicted in Fig. 2(c). Both the sensing and the exciting coil are wound around the inner magnetic core. The characteristics of the coils are also displayed in Table I, where R_s and R_e, and N_s and N_e are the resistance and the number of turns of the sensing and exciting coil accordingly. D_w is the wire diameter, which is identical for both coils. A plastic holder with round openings, which is depicted with white color in Fig. 2(c), was 3-D printed to keep the ferromagnetic inner and outer core of the valve together, as well as to allow the flow of MR fluid through the gap of the valve.

TABLE I: Magnetorheological module dimensions and coil characteristics

Quantity	Value
h	10 mm
h_t	2.5 mm
g	0.5 mm
r_i	8.83 mm
r_o	5 mm
R_s	2.75 Ω
R_e	3.53 Ω
N_s	135.5
N_e	174.5
D_w	0.224 mm

D. Experimental Sessions

The goal of this work was to validate the self-sensing properties of the MR valve with regard to pressure and correlate the applied pressure with the induced signal on the sensing coil of the valve. In order to achieve it, we needed to simulate the real condition of pressure applied to the MR fluid and the creation of flow through the gap of the valve. For this reason, we used the specially designed testbench of Fig. 3 that consists of the following parts: (i) two fluid chambers, one closed and one open; (ii) the MR valve placed in-between the two chambers; (iii) a pneumatic piston (SMC CDQ2A32TF-50DZ) that applies pressure on the fluid. The piston is placed in the closed chamber and creates a flow from the closed to the open chamber. A pneumatic valve, acting as a switch and controlled by an Arduino Uno, defines the movement of the piston; (iv) a laser displacement sensor (LK-G150 with LK-G3001PV all-in-one-controller) to measure the displacement of the pneumatic piston in each application of pressure.

In parallel, the exciting coil was supplied with a DC current, while the sensing coil was connected to an instrumentation amplifier with a gain of 500. The amplifier's output voltage was acquired with an oscilloscope (Teledyne LeCroy LT224). For our experimental sessions, the MR fluid MRF132DG [19] was used, which is commercially available by Lord Corporation. Compressed air was provided directly to the pneumatic piston through tubes.

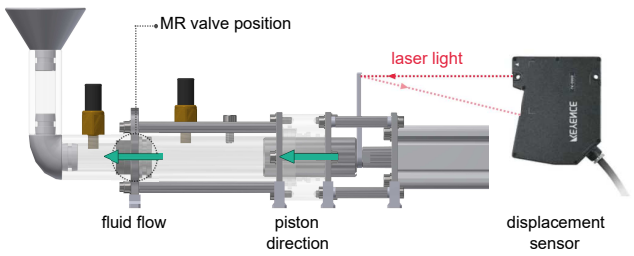

Fig. 3: The testing setup, with two chambers, a pneumatic piston for pressure application and flow creation and a laser displacement sensor.

III. Preliminary Results & Discussion

As explained previously, the MR valve functions in two states. In the closed state where high pressures can be sustained, the particles of the fluid chains are linked with strong bonds. In this case, it is hard to create an elongation of the chains with the application of pressure. Nevertheless, the existence of a current is mandatory for the voltage induction. In order to discover the ideal current value, which leads to the formation of chains but not too strong ones, we performed a series of measurements for different current values. Initially, we carried out measurements of the induced voltage on the sensing coil for several combinations of current and pressure. More specifically, as presented in Table II, the current ranged from $0.1\ A$ to $0.7\ A$ with a step of $0.1\ A$ and the pressure ranged from $100\ kPa$ to $700\ kPa$. We observed that for a current of $0.7\ A$ the induced voltage appeared only for very high pressures ($>= 600kPa$). This happens because the increase of current causes the creation of stronger particle chains, for which it is difficult to be elongated. The current testbench allows us to reach a maximum pressure of $700\ kPa$, with robust enough measurements, due to the length of the pneumatic piston and the supply of compressed air. With this testbench, we managed to acquire the first preliminary results that prove that this type of MR device can be used both as a valve and a pressure sensor.

TABLE II: Appearance of induced voltage for combinations of current and pressure

	0.1A	0.2A	0.3A	0.4A	0.5A	0.6A	0.7A
100kPa	yes	no	no	no	no	no	no
200kPa	yes	yes	yes	no	no	no	no
300kPa	yes	yes	yes	yes	no	no	no
400kPa	yes	yes	yes	yes	no	no	no
500kPa	yes	yes	yes	yes	yes	yes	no
600kPa	yes	yes	yes	yes	yes	yes	yes
700kPa	yes	yes	yes	yes	yes	yes	yes

Considering that for currents higher than $0.3\ A$ the measured pressure ranges decrease drastically, as well as the power consumption increases, we performed measurements for the three first values of current ($0.1\ A$, $0.2\ A$, and $0.3\ A$). The experimental session included three measurements per combination of current and pressure. The average voltage was calculated.

In each measurement, the same procedure was followed. Initially, the piston was activated and started pushing forward (direction to the left as in Fig. 3) at $t = 0.1\ s$ and for $\Delta t = 0.1\ s$, forcing the MR fluid to flow through the gap. At $t = 0.2s$ the piston stopped pushing, but its movement did not cease instantaneously. On the contrary, we observed a small retraction (movement towards the right direction). This happened due to the air bubbles trapped in the closed chamber of the testbench. As it is known, the air is compressible and the forward movement of the piston led to its compression. When the piston stopped moving, the air decompressed and forced back the piston creating a tiny displacement.

In Fig. 4 the voltage measurements on the sensing coil when following the above procedure are presented. It is clear that for each measurement, when the piston starts the forward movement, two voltage spikes appear. Firstly, the voltage increases and reaches a local maximum peak and then decreases and reaches a local minimum peak. The piston movement causes the chain elongation and, thus, the increase of the magnetic reluctance of the MR fluid in the gap. This is the reason behind the first spike. However, right after this phenomenon, the chain-like structures are reorganized in the gap space, to achieve a steady state. This leads to the subsequent decrease of the reluctance and the second successive spike in the graph. We can also observe that for the local minima of the second spike there is a slight time shift with the increase of pressure. The reason is that higher pressure cause more important rearrangements of the particles in the space of the gap, and, as a result, the achievement of a steady state is more difficult and needs more time. Finally, when the piston is blocked at $t = 0.2\ s$, the very small but abrupt backward movement of the piston caused by the compressed air increases again the chain length and creates a third voltage spike. In our case, we ignore this spike, since we do not know exactly the pressure applied due to the decompression of the air, and we focus on the first part of the signal.

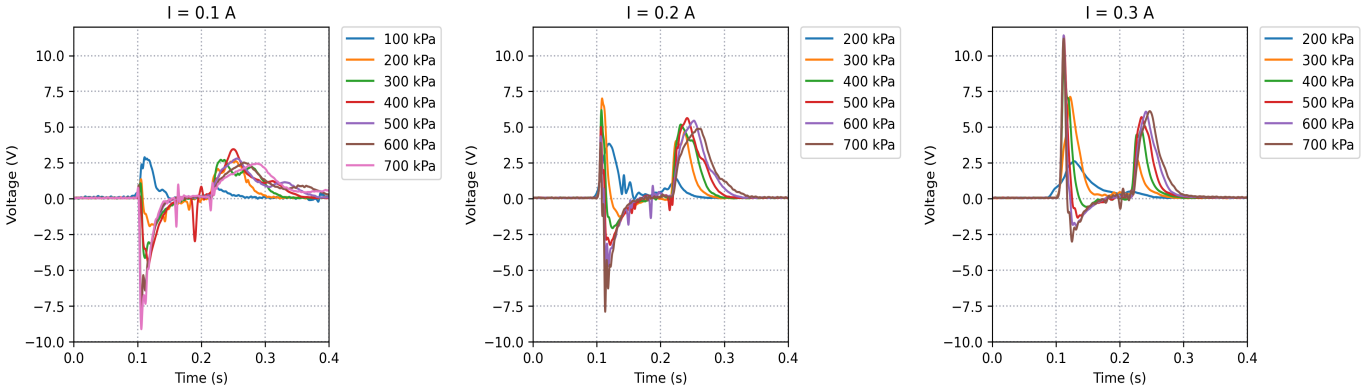

Fig. 4: Voltage measurements on the sensing coil of the MR valve for $0.1\ A$, $0.2\ A$ and $0.3\ A$ exciting current.

In Fig. 5, we depict the average minimum and maximum peaks for each current value in the range of pressure of $200\ kPa - 700\ kPa$. Regarding the maximum voltage peaks of the first spike, for currents of $0.1\ A$ and $0.2\ A$ there is no distinctive variation that could lead us to the extraction of useful information for pressure sensing. The lower current values create weaker chains that can be easily broken. Thus, the variation of the magnetic flux and reluctance in the gap is not distinguishable. Nevertheless, for the current of $0.3\ A$, we observe that there is an increase of the voltage with the increase of pressure and the voltage tends to stabilize for higher pressure.

The results are easier to interpret for the local minimum voltage values of the second spike, where a clear increase of the absolute value of voltage appears with the increase of pressure for all three current values. It is crucial to observe that the behavior of the voltage peaks is very close to linear, especially for the case of $0.3\ A$. This fact is promising for the future full characterization of MR actuator/sensor devices.

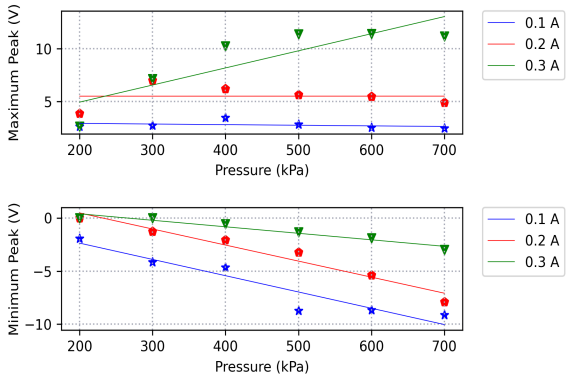

Fig. 5: Maximum and minimum voltage peaks, when the pneumatic piston is activated at $t = 0.1\ s$.

For the current design, further steps need to be followed to obtain the full characterization of a bifunctional MR valve. First of all, we must add pressure sensors to the fluid chambers, in order to control in parallel the pressure drop that arises on the two sides of the valve, and validate fully its simultaneous actuating purposes. Secondly, it will be useful to fabricate more valves with different dimensions, focusing on scaling down the current design, and acquire a robust enough induced voltage. The behaviors of all different-dimension valves can be compared, considering the applied current, the pressure range that can be measured for each design, as well as the induced voltage results. Finally, since the induced voltage appears when there exists a fluid flow, the valves can be studied about their self-sensing properties regarding displacement, velocity, and flow rate.

IV. Conclusions

In the current study, we fabricated and tested a miniature MR valve with a sensing and an exciting coil with regard to its pressure self-sensing properties. Using a specially designed testbench, we acquired induced voltages appearing on the sensing coil, due to the applied pressure on the fluid. The valve is powered only by a DC current both for the actuation and for the sensing mechanism, in comparison with the existing literature that uses also AC currents. It is the first time, that an MR valve is studied for its self-sensing properties regarding pressure in a range of pressures, proving there is a linear relationship between the applied pressure and the induced voltage. At the same time, it seems feasible for the valve to act as a sensor with low power consumption since the induced voltage can be sensed in a limited time while applying a low current value. The future steps include the integration of pressure drop measurements in parallel with voltage measurements, as well as the study of displacement, velocity, and flow rate self-sensing capabilities.

Acknowledgement

The authors acknowledge financial support from the BRIDGE funding programme, conducted by the Swiss National Science Foundation (SNSF) and Innosuisse–Swiss Innovation Agency.

References

[1] A. Pettersson, S. Davis, J. O. Gray, T. J. Dodd, and T. Ohlsson, “Design of a magnetorheological robot gripper for handling of delicate food products with varying shapes,” Journal of Food Engineering, vol. 98, no. 3, p. 332-338, 2010.

[2] A. Milecki, and M. Hauke, “Application of magnetorheological fluid in industrial shock absorbers,” Mechanical Systems and Signal Processing, vol. 28, pp. 528-541, 2012.

[3] T. Oba, H. Kadone, M. Hassan, and K. Suzuki, “Robotic Ankle–Foot Orthosis With a Variable Viscosity Link Using MR Fluid,” IEEE/ASME Transactions on Mechatronics, vol. 24, no. 2, p. 495-504, 2019.

[4] D. Case, B. Taheri, and E. Richer, “Dynamical modeling and experimental study of a small-scale magnetorheological damper,” IEEE/ASME Transactions on Mechatronics, vol. 19, no. 3, pp. 1015-1024, 2013.

[5] T. H. Yang, H. Son, et. al., “Magnetorheological Fluid Haptic Shoes for Walking in VR,” IEEE Transactions on Haptics, Early Access, 2020.

[6] T. Kikuchi, et al. “Torque-controllable device using a magnetorheological fluid with nano-sized iron particles for a haptic device,” IEEE International Conference on Advanced Intelligent Mechatronics (AIM), pp. 1154-1159, IEEE, 2017.

[7] F. Bucchi, P. Forte, F. Frendo, A. Musolino, and R. Rizzo, “A fail-safe magnetorheological clutch excited by permanent magnets for the disengagement of automotive auxiliaries,” Journal of Intelligent Material Systems and Structures, vol. 25, no. 16, p. 2102-2114, 2014.

[8] M. R. Jolly, J. D. Carlson, and B. C. Munoz, “A model of the behaviour of magnetorheological materials,” Smart Materials and Structures, vol. 5, no. 5, p. 607, 1996.

[9] S. Pisetskiy, and M. R. Kermani, “A Concept of a Miniaturized MR Clutch Utilizing MR Fluid in Squeeze Mode,” IEEE/RSJ International Conference on Intelligent Robots and Systems (IROS), pp. , IEEE, 2020.

[10] D. Case, B. Taheri, and E. Richer, “Dynamical modeling and experimental study of a small-scale magnetorheological damper,” IEEE/ASME Transactions on Mechatronics, vol. 19, no. 3, p. 1015-1024, 2013.

[11] M. Moghani, and M. R. Kermani, “Design and development of a hybrid magneto-rheological clutch for safe robotic applications,” IEEE International Conference on Robotics and Automation (ICRA), pp. 3083-3088, IEEE, 2016.

[12] C. Rossa, A. Jaegy, A. Micaelli, and J. Lozada, “Development of a multilayered wide-ranged torque magnetorheological brake,” Smart Materials and Structures, vol. 23, no. 2, p. 025028, 2014.

[13] S. L. Ntella, M. T. Duong, Y. Civet, Z. Pataky, and Y. Perriard, “Design optimization of miniature magnetorheological valves with self-sensing capabilities used for a wearable medical application,” IEEE/ASME International Conference on Advanced Intelligent Mechatronics (AIM), pp. 409-414, IEEE, 2020.

[14] F. Imaduddin, S. A. Mazlan, M. Rahman, H. Zamzuri, and B. Ichwan, "A high performance magnetorheological valve with a meandering flow path," Smart Materials and Structures, vol. 23, no. 6, p. 065017, 2014.

[15] G. Hu, W. Zhou, and W. Li, "A new magnetorheological damper with improved displacement differential self-induced ability," Smart Materials and Structures, vol. 24, no. 8, p. 087001, 2015.

[16] D. Wang and T. Wang, "Principle, design and modeling of an integrated relative displacement self sensing magnetorheological damper based on electromagnetic induction," Smart Materials and Structures, vol. 18, no. 9, p. 095025, 2009.

[17] D.-H. Wang and X.-X. Bai, "A magnetorheological damper with an integrated self-powered displacement sensor," Smart Materials and Structures, vol. 22, no. 7, p. 075001, 2013.

[18] D. Grivon, Y. Civet, Z. Pataky, and Y. Perriard, "Detection of pressure or flow rate variations in MR valves through magnetic flux analysis," 19th International Conference on Electrical Machines and Systems (ICEMS), pp. 1-5, IEEE, 2016.

[19] Lord Corporation, "Data Sheet - MRF-132DG Magneto-Rheological Fluid," http://www.lordmrstore.com/_literature_231215/data_sheet_-_mrf-132dg_magneto-rheological_fluid, 2021.